

Universal Quantum Erasing for Continuous Variables

Yoshichika Miwa,¹ Jun-ichi Yoshikawa,¹ Ryuji Ukai,¹ Radim Filip,² and Akira Furusawa¹

¹*Department of Applied Physics, School of Engineering, The University of Tokyo,
7-3-1 Hongo, Bunkyo-ku, Tokyo 113-8656, Japan*

²*Department of Optics, Palacký University, 17. listopadu 50, 772 07 Olomouc, Czech Republic
(Dated: January 23, 2019)*

We demonstrate continuous-variable analog of quantum erasing, which corresponds to undoing quantum nondemolition (QND) interaction. The QND interaction entangles two input states. Each state is decohered by the interaction because the information about one variable from one of two inputs (signal) is copied to the other input (probe). After the information transfer we erase the information via measurement of the probe, and then we completely restore the initial signal state with feedforward in principle. The quantum eraser is universal, i.e., it works equally for arbitrary input state. To verify the performance, we use a coherent state and a squeezed vacuum state as the input states. We verify erasure of the information by using the uncertainty relation between conjugate-variable measurements. In one-way quantum computation, the erasing operation corresponds to removing an unwanted mode from a cluster state, and repetition of the operations would enable us to flexibly shape the cluster state.

PACS numbers: 03.67.Lx, 42.50.Dv, 42.50.Ex

I. INTRODUCTION

Quantum erasing was originally proposed in the context of quantum complementarity and reversibility of decoherence [1]. In traditional double-slit-based experiment, the complementarity is written as a trade-off between which-way information and fringe visibility [2, 3]. Generally speaking, the decoherence is induced by interaction between a quantum system and its environment as a result of copying information of the quantum system to the environment. In the double-slit experiment, the information about a single variable—the path which photon has taken, is non-demolitionably transferred to environment. In the case of this specific non-demolishing interaction, proper measurement of the environment can erase the information and reverse the decoherence. Until now, most of quantum erasers are proposed and demonstrated with qubits [1, 4]. These qubit erasers deal with an entangled pair in which the information of one of two qubits can be interpreted to be copied to the other by a controlled-NOT operation. An interesting property of these quantum erasers is that reversing the decoherence or reconstruction does not depend on a state of the environment (even arbitrary noisy) [5]. No special condition of the environment is required to approach the perfect reconstruction. On the other hand, continuous-variable (CV) quantum erasing reverses the decoherence induced by a quantum non-demolition (QND) interaction [6, 7].

A typical qubit eraser works as follows. Here “signal” and “probe” are a quantum system and its environment, which are denoted by the subscripts “S” and “P”, respectively. Suppose the initial signal state is $|\pm\rangle_S$, i.e. either $|+\rangle_S$ or $|-\rangle_S$, where $|\pm\rangle = \frac{1}{\sqrt{2}}(|0\rangle \pm |1\rangle)$ is a superposition of $|0\rangle$ and $|1\rangle$ which are orthogonal computational-basis (CB) eigen states. Then, the signal qubit is entangled with the probe qubit in $|0\rangle_P$ or alternatively $|1\rangle_P$ via a controlled-NOT operation [8]. The resulting state is a fully entangled state $|\Psi\rangle_{SP} = \frac{1}{\sqrt{2}}(|0\rangle_S|0\rangle_P \pm |1\rangle_S|1\rangle_P)$, or alternatively $|\Psi\rangle_{SP} = \frac{1}{\sqrt{2}}(|0\rangle_S|1\rangle_P \pm |1\rangle_S|0\rangle_P)$. Now the state of signal qubit is decohered and becomes a fully

mixed state when we consider only the signal qubit. Here the density operator is $\hat{\rho}_S = \frac{1}{2}(|0\rangle_S\langle 0| + |1\rangle_S\langle 1|)$ for all the cases above, which is derived via tracing out the probe qubit. The controlled-NOT operation can be interpreted as perfectly copying the signal which-CB “information” to the probe qubit. This *leaking information* collapses the superposition, even without any measurement, and the resulting signal qubit state is incoherent mixture of $|0\rangle_S$ and $|1\rangle_S$. By erasing the *leaking information*, we can reverse the decoherence. This is done by making a measurement in a superposition basis $|\pm\rangle_P$ because the measurement reveals the *complementary information* and disenables us to access the *leaking information*. The measurement results in preserving superposition in the signal qubit as $|\pm\rangle_S$ in the case of $|+\rangle_P$, or $|\mp\rangle_S$ in the case of $|-\rangle_P$. In order to restore the initial qubit states $|\pm\rangle_S$, we perform a feed-forward correction, namely making unitary transformation $|\pm\rangle_S \rightarrow |\mp\rangle_S$ if the state $|-\rangle_P$ has appeared. Note that this feedforward does not depend on whether the initial probe state is $|0\rangle_P$ or $|1\rangle_P$. Generally speaking, the erasing procedure is universal, i.e., it works for any unknown input states of signal and probe, even if there is no entanglement after the controlled-NOT operation [5].

Mechanism of a CV eraser well corresponds to that of the qubit eraser. Instead of $|0\rangle$ and $|1\rangle$ for a qubit, coordinate eigenstates $|x\rangle$ for any real number x are the CB in the CV case. Suppose initial signal state is $|\psi\rangle_S = \int dx \psi(x) |x\rangle_S$ as a superposition of the CB. Then, the signal mode is entangled with the probe mode by a QND interaction, where its unitary operator is $\hat{U} = \exp(i\hat{x}_S\hat{p}_P/\hbar)$. Similarly as for the discrete case, the QND interaction transfers information only in the single variable. Although initial probe state is arbitrary for CV quantum erasing, we assume $|0\rangle_P$ for simplicity here. Later, we describe the general case. In the case of $|0\rangle_P$, the output state is $|\Psi\rangle_{SP} = \int dx \psi(x) |x\rangle_S |x\rangle_P$. The signal-coordinate *information* is completely copied to the probe by the QND interaction. Thus, the state of the signal mode becomes a mixed state whose density operator is $\hat{\rho}_S = \int dx |\psi(x)|^2 |x\rangle_S\langle x|$. Information transfer to the probe mode in the coordinate basis

collapses the superposition, and the resulting signal state is a coordinate eigen state $|x\rangle_S$, which is known as a QND measurement. In contrast, measurement on the momentum basis erases the *information* and the coherence of the signal mode is restored. This is because the coordinate and momentum operators are conjugate to each other. The eraser can also restore the unknown initial state $|\psi\rangle_S$ with proper feedforward, while experimental qubit erasers are usually evaluated only on recovery of the coherence [1, 4].

It is known that there is a trade-off between the *information* and the decoherence. For qubits, in the traditional double-slit-based model, the trade-off originates from wave-particle duality and is written as the relation between which-way information and fringe visibility [2, 3]. For CV cases, the trade-off originates from the uncertainty principle. In the above case of CV, we have considered the extreme case which gives maximum *information* and maximum decoherence, by supposing $|0\rangle_P$ is the initial probe state. When we use states other than $|x\rangle_P$, the QND measurement with finite precision is achieved, resulting in smaller decoherence. Here the decoherence on the coordinate basis can be observed as increase of the momentum variance, which corresponds to back action of the QND measurement. The uncertainty relation between the QND-measurement accuracy and the back action is [9],

$$\Delta x_{\text{error}} \Delta p_{\text{back action}} \geq \frac{1}{4}, \quad (1)$$

as derived later, where the commutation relation of coordinate and momentum operators is $[\hat{x}, \hat{p}] = i/2$ with normalization $\hbar = 1/2$, and where Δx_{error} and $\Delta p_{\text{back action}}$ denote the QND measurement error and back action as standardized deviations. Thus, the minimal back action is $\Delta p_{\text{back action}}^{\text{min}} = 1/(4\Delta x_{\text{error}})$.

After a perfect quantum erasing operation, the back action is completely removed, i.e., $\Delta p_{\text{residual noise}} = 0$. In experiments, there is some residual noise after the erasing operation due to experimental imperfections, however, the *information* should be partly erased if the residual noise is below the minimal back action, i.e., $\Delta p_{\text{residual noise}} < \Delta p_{\text{back action}}^{\text{min}}$, or equivalently,

$$\Delta x_{\text{error}} \Delta p_{\text{residual noise}} < \frac{1}{4}. \quad (2)$$

We consider Ineq. (2) as a sufficient condition for the success of quantum erasing. Note that this relation does not conflict with Ineq. (1) because those two amounts Δx_{error} and $\Delta p_{\text{residual noise}}$ can not be obtained simultaneously.

The quantum erasing operation is not only of theoretical interest but also an indispensable tool for shaping cluster states in one-way quantum computation [10]. A one-way quantum computer requires a resource cluster state, where a qubit (CV) cluster state has graph structure where the nodes are qubits (quantum modes) while the bonds represent controlled π -phase-shift (controlled-Z) interactions [11, 12]. By Hadamardt (Fourier) transformations, these interactions become controlled-NOT (QND) interactions, and therefore, quantum erasers can cut the bonds and remove unwanted

qubits (modes) from the cluster state. Quantum erasers provide flexibility of fixed large-scale cluster states proposed in Ref. [13], and enable us to shape and convert the cluster states into modified, smaller cluster states suitable for given quantum computation tasks [10, 14].

In this paper, we demonstrate universal CV quantum erasing as undoing a QND interaction. Here, the first experimental CV quantum eraser reported in Ref. [15] utilizes a beam-splitter interaction instead of the QND interaction. However, the beam-splitter interaction cannot be undone by measurement-based protocol mentioned above. For that reason, their scheme requires $|0\rangle$ as the initial probe state, and the resulting state is unavoidably squeezed. Without probe squeezing, the quantum erasing requires measurement of both the variables, which leads only to limited reconstruction of the input state [16]. In contrast, with a QND interaction, we can restore any initial signal state, and the resulting state does not depend on the initial probe state. We verify quantum states of the signal and probe throughout the process by performing homodyne tomography.

II. THEORY

Figure 1(i) shows a schematic of CV quantum erasing. Input quantum states of signal and probe modes are independently prepared (a), and then a QND interaction couples them (b), finally, measurement and feedforward restore the initial signal state (c). During the scheme in Fig. 1(i), the signal and probe quantum states change through the following three steps (a), (b), and (c). Hereafter, we describe quantum states in these steps denoted by superscripts (a), (b), and (c) and derive the uncertainty relation of Ineq. (1).

The states $|\psi\rangle_S$ and $|\phi\rangle_P$ represent arbitrary initial quantum states of the signal and probe modes, respectively. In order to deal with nonmaximally entangled and separable cases, we do not assume $|\phi\rangle = |0\rangle$ here as we do in the introduction. These modes are entangled by the QND interaction. The output entangled state is

$$\begin{aligned} |\Psi^{(b)}\rangle &= e^{2i\hat{x}_S\hat{p}_P} |\psi\rangle_S |\phi\rangle_P \\ &= \iint dx_S dx_P |x_S\rangle_S |x_P + x_S\rangle_P \psi(x_S) \phi(x_P) \end{aligned} \quad (3)$$

$$= \iint dp_S dp_P |p_S - p_P\rangle_S |p_P\rangle_P \tilde{\psi}(p_S) \tilde{\phi}(p_P), \quad (4)$$

where $\psi(x_S) \equiv \langle x_S | \psi \rangle$ and $\phi(x_P) \equiv \langle x_P | \phi \rangle$ are the input wave functions on coordinate bases of the signal and probe, respectively, while $\tilde{\psi}(p_S) \equiv \langle p_S | \psi \rangle$ and $\tilde{\psi}(p_P) \equiv \langle p_P | \phi \rangle$ are the input wave functions on momentum bases, which are obtained by the Fourier transformation denoted by “ \sim ” via $\langle x | p \rangle = e^{i2xp} / \sqrt{\pi}$. Obviously, the entangled state has correlation in both coordinate and momentum observables represented in Eqs. (3) and (4).

The state in each mode is derived by tracing out the other

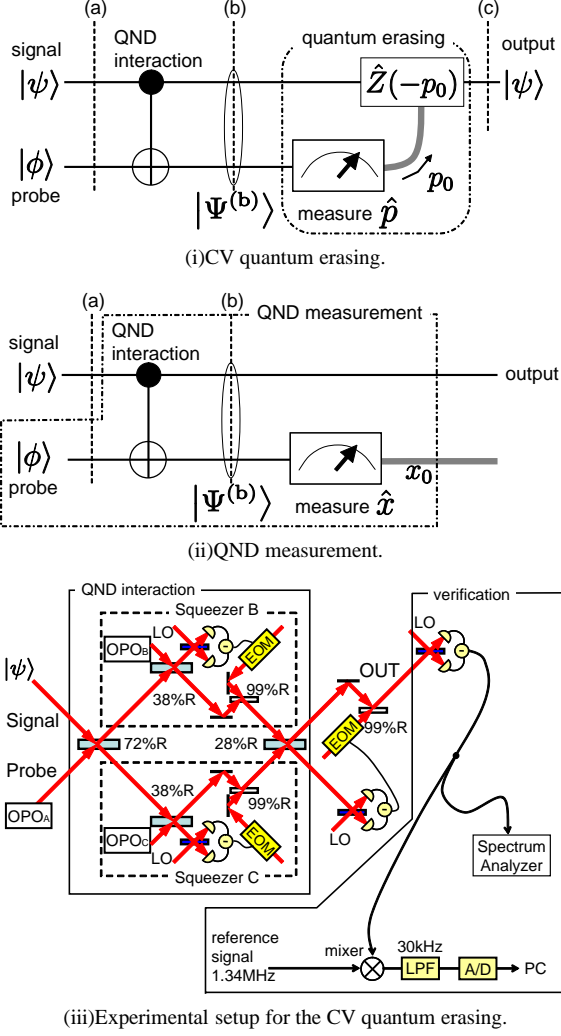


FIG. 1: (Color online) Schematic and our optical setup of CV quantum erasing. OPO: optical parametric oscillator, LO: optical local oscillator, and EOM: electro-optic modulator.

mode as following density operators:

$$\hat{\rho}_S = \iint dx dx' |x\rangle_S \langle x'| \psi(x) \psi^*(x') R_{\phi\phi}(x' - x), \quad (5)$$

$$= \iint dp dp' |p\rangle_S \langle p'| [\tilde{\psi}(p) \circ \tilde{\phi}(-p)] [\tilde{\psi}^*(p') \circ \tilde{\phi}^*(-p')], \quad (6)$$

$$\hat{\rho}_P = \iint dx dx' |x\rangle_P \langle x'| [\phi(x) \circ \psi(x)] [\phi^*(x') \circ \psi^*(x')], \quad (7)$$

$$= \iint dp dp' |p\rangle_P \langle p'| \tilde{\phi}(p) \tilde{\phi}^*(p') R_{\tilde{\psi}\tilde{\psi}}(p - p'), \quad (8)$$

where “*” and “o” denote complex conjugate and convolution, respectively, and $R_{\phi\phi}(x)$ represents autocorrelation coefficient of ϕ with the coordinate shift of x , $R_{\phi\phi}(x) = \phi(x) \circ \phi^*(-x)$.

Intuitively speaking, Eq. (5) represents the decoherence on the coordinate basis of the signal, which corresponds to the

back action in momentum as shown in Eq. (6). Eq. (7) represents that the probe state has the *information* of the signal coordinate. The autocorrelation function satisfies $R_{\phi\phi}(0) = 1$ and $|R_{\phi\phi}(x)| < 1$ for $x \neq 0$, except for some unphysical states such as $|\phi\rangle = |p = p_0\rangle$ for any real p_0 . By applying these features of the autocorrelation to Eq. (5), we can derive that the diagonal elements of signal density matrix on the coordinate basis are preserved through the QND interaction, while the off-diagonal elements become smaller in absolute value. Therefore, the distribution of x_S is preserved, while the superposition is decohered. The same things occur on the probe momentum as represented in Eq. (8). On the other bases, namely the signal momentum and the probe coordinate, these density matrices become convolutions of two initial wave functions as represented in Eqs. (6) and (7). In the QND measurement [Fig. 1(ii)], these convolutions show that both the measurement back action ($\Delta p_{\text{back action}}$) and the measurement error (Δx_{error}) depend on $\phi(x)$ and $\phi(p)$, while, the variances of these wave functions cannot be suppressed simultaneously. Thus, the uncertainty relation in Ineq. (1) can be derived.

After the QND interaction, \hat{p}_P is measured for quantum erasing. With the measurement result of p_0 in Eq. (4), we calculate that the signal state is projected to

$$\int dp_S |p_S - p_0\rangle \tilde{\psi}(p_S) \tilde{\phi}(p_0) = \tilde{\phi}(p_0) \int dp_S |p_S - p_0\rangle \tilde{\psi}(p_S) \propto \hat{Z}(-p_0) |\psi\rangle_S, \quad (9)$$

where \hat{Z} is a phase-space displacement operator. By performing feedforward in order to cancel the phase-space displacement $\hat{Z}(-p_0)$, the initial signal state $|\psi\rangle$ is restored. Since the erasing operation works for any basis states, it also works for any mixed initial states of signal and probe.

Here, the *information* of signal wave function is concealed throughout the process because the measurement result p_0 does not reflect any property of the initial signal state as denoted in Eq. (8). Besides, the measurement of \hat{p}_P erases the *information* from \hat{x}_P owing to their conjugateness. Therefore, the decoherence of the signal disappears together with the *information*. Furthermore, there are no assumptions on the initial signal and probe states. Thus, the quantum erasing operation restores an arbitrary initial signal state just like quantum teleportation. Note that, for the teleportation, the signal and probe correspond to the input and resource, respectively, while, for quantum erasing, the signal and probe are interchangeable and both states are arbitrary. In this sense, the quantum erasing and teleportation are different, where erasing undoes a QND interaction, while teleportation does not.

III. EXPERIMENTAL SETUP

Figure 1(iii) shows our optical implementation of Fig. 1(i). The experimental setup consists of the following parts: preparation of the input signal and probe states, QND interaction [17], measurement, feedforward, and, finally, the verification measurement. This setup is similar to that of our

quadratic phase gate [18]. However, since the quadratic phase gate is generalized teleportation [18], it requires a squeezed vacuum state as the initial probe state, while the quantum erasing operation does not depend on the initial probe state. Besides, the mode to be measured and the mode to be suffered from feedforward are also different between these two operations.

As a light source, we utilize a continuous-wave Ti:sapphire laser with the wave length of 860 nm. As signal input state, a coherent state at the 1.34 MHz sideband is generated by modulating a weak laser beam of about $10 \mu\text{W}$ using two electro-optic modulators (EOMs). One of the EOMs modulates the phase of the beam and the other modulates the amplitude, where coordinate x and momentum p correspond to these amplitude and phase quadratures respectively in our optical implementation. Thus, these two EOMs can generate a coherent state with any complex amplitude from the laser beam.

In order to prepare the probe input state and resource squeezed-vacuum states for QND interaction, we utilize three sub-threshold optical parametric oscillators (OPOs), each generating a single-mode squeezed state, whose squeezing level is about -5 dB relative to the shot-noise level (SNL). Each OPO is a bow-tie shaped cavity of 500 mm in length with a 10-mm-long PPKTP crystal as a nonlinear medium [19]. The second harmonic (430 nm in wavelength) of Ti:sapphire output is divided into three beams in order to pump the OPOs.

The QND interaction consists of a Mach-Zehnder interferometer with a single-mode squeezing gate in each arm [17]. Each single-mode squeezing gate contains a squeezed vacuum ancilla, homodyne detection, and feedforward [20, 21]. Four beam splitters with reflectivities of 72%, 38%, 38%, 28% are implemented as variable beam splitters (VBSs), each composed of two polarizing beam splitters and a half-wave plate. These four reflectivities are chosen to achieve unity gain QND interaction [17]. For reference, we can eliminate the QND interaction and just measure input states by setting the reflectivities of these VBSs to unity. Moreover, we can easily exchange the signal and probe outputs of QND interaction by adjusting the reflectivity of the fourth VBS to 72%. At each beam splitter, we lock the relative phase of the two input beams by means of active feedback to a piezoelectric transducer. For this purpose, two modulation sidebands of 154 kHz and 107 kHz are used as phase references.

To verify the output state, we employ another homodyne detection. For accurate evaluation of variance in x or p -quadrature, we lock the optical local oscillator (LO) phase and extract 1.34 MHz component of the measurement outcome via a spectrum analyzer. Meanwhile, in order to reconstruct the resulting quantum state, we perform optical homodyne tomography, namely, quantum state reconstruction from the marginal distributions for various phases [22]. We slowly scan through the LO phase and perform a series of homodyne measurements. The 1.34 MHz component of the homodyne signal is extracted by means of lock-in detection: it is mixed with a reference signal and then sent through a 30 kHz low pass filter. Finally, it is digitized with the sampling rate of 300,000 samples per second.

The powers of the LOs are about 3 mW. The detector's

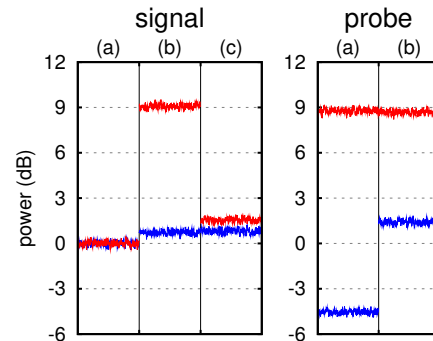


FIG. 2: (Color) Experimental results of variances in each stage / mode of Fig. 1(i) relative to the shot-noise limit. Each red trace represents variance of p -quadrature while each blue trace represents x -quadrature. Initial signal and probe states are a vacuum state and a squeezed vacuum state (a), the signal variance of x -quadrature is added to the probe x -quadrature while the back action appears in the signal p -quadrature owing to a QND interaction (b), the back action is reduced by measuring p -quadrature of the probe and performing feedforward (c).

quantum efficiencies are greater than 99%, the interference visibilities to the LOs are on average 98%, and the circuit noise of each homodyne detector is about 17 dB below the SNL produced by the LO. Propagation losses of our whole setup are about 7%. Experimental QND gains are about 0.99, where the losses mentioned above are compensated via the equality of losses between inputs and outputs.

IV. EXPERIMENTAL RESULTS

First, we evaluate variances of input and output states of the QND interaction or a quantum eraser to verify the erasure of the *information*. Here, we put a vacuum state as an initial signal state, and then we measure the powers with homodyne detectors and a spectrum analyzer. Figure 2 shows experimental results of these variances. We obtained the variance of probe- x -quadrature $V_p^{(b)}(x) = 0.346 \pm 0.006$ after the QND interaction, the variance of signal- p -quadrature $V_s^{(b)}(p) = 2.02 \pm 0.03$ after the QND interaction, and the one $V_s^{(c)}(p) = 0.358 \pm 0.005$ after quantum erasing. Here, $1/4 = 0.25$ of each variance corresponds to the initial signal state. Subtracting the variance of input vacuum state ($1/4 = 0.25$) from these variances, we obtain measurement error of a QND measurement $(\Delta x_{\text{error}}^{(b)})^2 = 0.096 \pm 0.006$ and its back action $(\Delta p_{\text{back action}}^{(b)})^2 = 1.77 \pm 0.03$ while quantum erasing suppress the back action quite well to be $(\Delta p_{\text{residual noise}}^{(c)})^2 = 0.108 \pm 0.005$. Thus, in the case of the QND measurement, Ineq. (1) is satisfied,

$$\Delta x_{\text{error}}^{(b)} \Delta p_{\text{back action}}^{(b)} = 0.414 \pm 0.016 \geq \frac{1}{4}. \quad (10)$$

Note that the uncertainty is not minimum, which is mainly caused by using a mixed state, namely a squeezed thermal

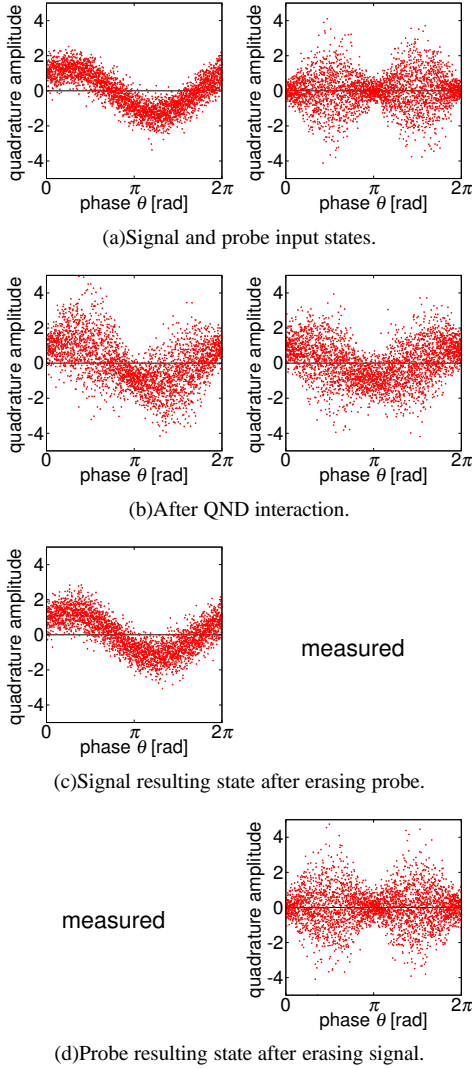


FIG. 3: (Color online) Experimental marginal distribution in each stage / mode of quantum erasing. Left-side figures are marginal distributions of signal mode and right-side ones are those of probe mode. The signal (probe) is initially a coherent (squeezed-vacuum) state (a). The QND interaction induces decoherence in the signal and probe (b). Erasing the probe (signal) mode, the initial signal (probe) state is recovered (c) [(d)].

state, as the initial probe state. On the other hand, in the case of quantum erasing, the back action is suppressed below the *information erasure* criteria of Ineq. (2),

$$\Delta x_{\text{error}}^{(b)} \Delta p_{\text{residual noise}}^{(c)} = 0.102 \pm 0.006 < \frac{1}{4}. \quad (11)$$

Therefore, the *information* of the signal is successfully erased. Note that the residual noise mainly comes from finitely squeezed ancillas of the QND interaction [17, 20].

Next, we evaluate the performance of the setup for an input with coherent amplitude in order to verify the preservation of the amplitude throughout the process. We put a coherent (squeezed vacuum) state as the initial signal (probe) state and examine the states throughout the process via homodyne to-

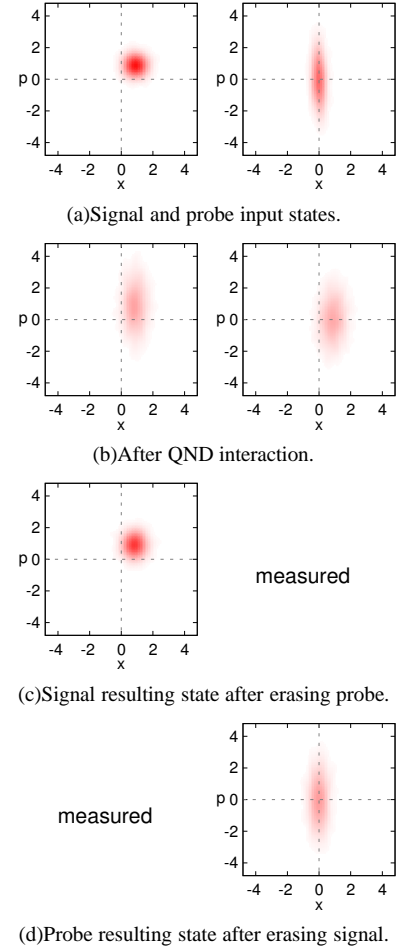


FIG. 4: (Color online) Reconstructed Wigner functions from experimental marginal distributions shown in Fig. 3. Left-side figures are Wigner functions of signal mode and right-side ones are those of probe mode. The signal (probe) is initially a coherent (squeezed-vacuum) state (a). The QND interaction induces decoherence in the signal and probe (b). Erasing the probe (signal), the initial signal (probe) state is recovered (c) [(d)].

mography. Figure 3 shows raw data of marginal distributions, while Fig. 4 shows reconstructed Wigner functions using maximum likelihood method [22, 23]. Input coherent state (a) of the signal becomes a mixed state (b) because of the QND interaction with the probe mode. The amplitude and variance of x -quadrature (corresponds to LO phase $\theta = 0, \pi$) are almost preserved and they are reflected in the probe x -quadrature after the QND interaction in which the information of signal is copied to the probe. The mean amplitude of p -quadrature ($\theta = \pi/2, 3\pi/2$) is also well-preserved, while the variance of p -quadrature is enlarged due to the back action. After the erasing operation (c), the noise in p -quadrature is well suppressed, and thus, the input state is restored. Although there is excess noise coming from imperfections of QND interaction, the fidelity (overlap between input and output state) was very high, $\langle \psi^{(a)} | \rho^{(c)} | \psi^{(a)} \rangle = 0.85 \pm 0.02$.

Furthermore, we perform the erasing operation with exchanging the signal and probe state in order to verify that it

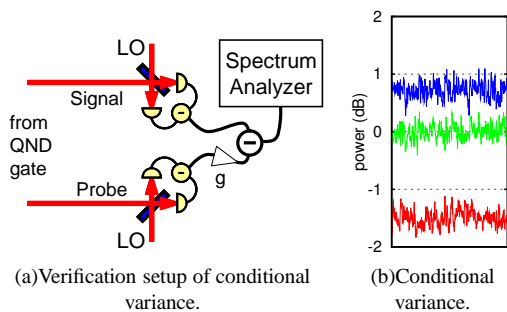


FIG. 5: (Color) Verification setup and experimental results of conditional variance of the signal x -quadrature when the probe x -quadrature is measured. Here both the signal and probe are measured via homodyne-detectors, their outcomes are electrically subtracted in the optimal gain $g = 0.56$ and measured by spectrum analyzer. The signal x -quadrature variance (green trace) is reduced by measuring x -quadrature of probe (red), and suppressed below the shot-noise limit (blue).

is applicable to a squeezed signal state and it does not depend on the probe state. In this case, the initial squeezed vacuum state (a) becomes a mixed state (b) due to the QND interaction with a coherent state, and then, the squeezed vacuum state is restored (d) by quantum erasing as shown in Figs. 3 and 4. Here, the decoherence occurs on amplitude reflecting the input coherent state, and it disappears after the erasing operation. This clearly shows the expected feature that the resulting state after erasing is independent of the initial probe state, unlike the experiment in Ref. [15]. The variance of the squeezed quadrature of each stage [(a), (b), and (d)] is -4.9 ± 0.2 dB, 1.5 ± 0.2 dB and -1.0 ± 0.2 dB relative to the SNL, showing that non-classical property is recovered by quantum erasing, even with a coherent-state probe.

For verification of our QND interaction, we evaluate the performance of a QND measurement with the criteria proposed in Ref. [24]. Here, we put a vacuum state as an initial signal state, and then we measure variances with homodyne detectors and a spectrum analyzer. As already mentioned, measurement error $(\Delta x_{\text{error}}^{(b)})^2$ was only 0.096 ± 0.006 . The QND variable x_S is well preserved with in the variance $V_S^{(b)}(x) = 0.295 \pm 0.004$ as shown in Fig. 2. The verification setup represented in Fig. 5(a) yields conditional variance (Fig. 5(b)),

$$V_{S|P} = \min_g \langle V(\hat{x}_S - g\hat{x}_P) \rangle = 0.177 \pm 0.003 < \frac{1}{4}, \quad (12)$$

which is suppressed below the SNL. Thus, there exists non-classical correlation between the signal and probe quadratures. These results satisfy the QND-measurement criteria. Furthermore, by adjusting subtracting gain g in Eq. (12) to unity i.e. $g = 1$, we also evaluate the entanglement between the signal and probe after the QND interaction. We obtained the correlation of x quadratures $V(\hat{x}_S - \hat{x}_P) = 0.243 \pm 0.003 < 1/2$ and the one of p quadratures $V(\hat{p}_S + \hat{p}_P) = 0.341 \pm 0.003 < 1/2$, which satisfy the Duan-Simon entanglement criteria [25, 26]. Therefore, our QND interaction satisfies the QND and entangling criteria. So we can conclude that our quantum eraser is undoing such an appropriate QND interaction.

In conclusion, we have experimentally demonstrated universal CV quantum erasing as undoing a QND interaction. To verify that the quantum erasing works equally for arbitrary input states, we have used a coherent state and a squeezed vacuum state as input states. We have entangled them by the QND interaction, and then observed that each state is decohered owing to copying the information by the interaction. After that, we have restored either of the two input states. An initial coherent state has been restored with 86% fidelity which is verified by homodyne tomography. A squeezed-vacuum state has also been restored, which shows the erasing operation can recover non-classical properties. We have verified erasure of the information by using the uncertainty relation between conjugate-variable measurements. In one-way quantum computation, repetition of this operation would enable us to shape a fixed large-scale cluster state to a suitable shape for a given quantum computing task.

Acknowledgement

This work was partly supported by SCF, GIA, G-COE, PFN and FIRST commissioned by the MEXT of Japan, the Research Foundation for Opt-Science and Technology, SCOPE program of the MIC of Japan, and, JSPS and ASCR under the Japan-Czech Republic Research Cooperative Program. R. F. acknowledges projects: MSM 6198959213 and ME10156 of the Czech Ministry of Education, grant 202/08/0224 of GA ĀR and EU Grant FP7 212008 COMPAS.

[1] M. O. Scully and Kai Drühl, Phys. Rev. A **25**, 2208 (1982).
 [2] G. Jaeger, A. Shimony, and L. Vaidman, Phys. Rev. A **51**, 54 (1995).
 [3] B.-G. Englert, Phys. Rev. Lett. **77**, 2154 (1996).
 [4] Y.-H. Kim, R. Yu, S. P. Kulik, Y. Shin, and M. O. Scully, Phys. Rev. Lett. **84**, 1 (1999).
 [5] P. D. D. Schwindt, P. G. Kwiat, and B.-G. Englert, Phys. Rev. A **60**, 4285 (1999).

[6] R. Filip, J. Opt. B **4**, 202 (2002).
 [7] R. Filip, Phys. Rev. A **67**, 042111 (2003).
 [8] M.A. Nielsen and I.L. Chuang, Quantum Computation and Quantum Information, Cambridge University Press, ISBN 0-521-63235-8 (2000).
 [9] V. B. Braginsky and F. Y. Khalili, *Quantum measurement* (Cambridge University Press, Cambridge, 1992).
 [10] Y. Miwa, R. Ukai, J. Yoshikawa, R. Filip, P. van Loock, and A.

- Furusawa, arXiv:1006.2225 [quant-ph] (2010).
- [11] R. Raussendorf, D. E. Browne, and H. J. Briegel, *Phys. Rev. A* **68**, 022312 (2003).
 - [12] N. C. Menicucci, P. van Loock, M. Gu, C. Weedbrook, T. C. Ralph, and M. A. Nielsen, *Phys. Rev. Lett.* **97**, 110501 (2006).
 - [13] N. C. Menicucci, S. T. Flammia, and O. Pfister, *Phys. Rev. Lett.* **101**, 130501 (2008).
 - [14] M. Gu, C. Weedbrook, N. C. Menicucci, T. C. Ralph, and P. van Loock, *Phys. Rev. A* **79**, 062318 (2009).
 - [15] U. L. Andersen, O. Glöckl, S. Lorenz, G. Leuchs, and R. Filip, *Phys. Rev. Lett.* **93**, 100403 (2004).
 - [16] M. Sabuncu, R. Filip, and G. Leuchs, and U. L. Andersen, *Phys. Rev. A* **81**, 012325 (2010).
 - [17] J. Yoshikawa, Y. Miwa, A. Huck, U. L. Andersen, P. van Loock, and A. Furusawa, *Phys. Rev. Lett.* **101**, 250501 (2008).
 - [18] Y. Miwa, J. Yoshikawa, P. van Loock, and A. Furusawa, *Phys. Rev. A* **80**, 050303(R) (2009).
 - [19] S. Suzuki, H. Yonezawa, F. Kannari, M. Sasaki, and A. Furusawa, *Appl. Phys. Lett.* **89**, 061116 (2006).
 - [20] R. Filip, P. Marek, and U.L. Andersen, *Phys. Rev. A* **71**, 042308 (2005).
 - [21] J. Yoshikawa, T. Hayashi, T. Akiyama, N. Takei, A. Huck, U.L. Andersen, and A. Furusawa, *Phys. Rev. A* **76**, 060301(R) (2007).
 - [22] A. I. Lvovsky and M.G. Raymer, *Rev. Mod. Phys.* **81**, 299 (2009).
 - [23] A. I. Lvovsky, *J. Opt. B* **6**, S556 (2004).
 - [24] M. J. Holland, M. J. Collett, and D. F. Walls, and M. D. Levenson, *Phys. Rev. A* **42**, 2995 (1990).
 - [25] L.-M. Duan, G. Giedke, J.I. Cirac, and P. Zoller, *Phys. Rev. Lett.* **84**, 2722 (2000).
 - [26] R. Simon, *Phys. Rev. Lett.* **84**, 2726 (2000).